

FIBER TRACKING OF HUMAN BRAIN USING MOMENT-BASED ORIENTATION DISTRIBUTION FUNCTION AND MULTI-SHELLED Q-BALL IMAGING

E. Umezawa¹, Y. Kuwayama², A. Yamamoto², H. Masumoto², T. Fukuba², M. Ohashi², K. Terada², T. Mori², Y. Kinomura², K. Yamaguchi¹, M. Yamada¹, H. Anno¹, and K. Katada³

¹School of Health Sciences, Fujita Health University, Toyoake, Aichi, Japan, ²Radiological Division, Fujita Health University Hospital, Toyoake, Aichi, Japan, ³Department of Radiology, School of Medicine, Fujita Health University, Toyoake, Aichi, Japan

Introduction: q-Space imaging (QSI) is a promising candidate that solves the crossing fiber problem in the diffusion tensor imaging. This method gives the probability density function (PDF) (1) that has information to give the intravoxel multi-fiber orientations. This requires, however, time intensive 3D q-space samplings. q-Ball imaging (QBI) gives an orientation distribution function (ODF) by sampling only on a spherical shell in q-space (2). Although the information of ODF is less than that of PDF, ODF enable us to identify the intravoxel multi-fiber orientations. The local maxima of ODF are assumed to indicate the fiber orientations. If two fibers cross with an acute angle, however, the ODF-estimated angle is smaller than the actual angle (3). We have proposed a novel method (Multi-Shelled QBI (MS-QBI)) that gives a new ODF based on the moment of PDF (4). In the conventional QSI, the moments are calculated using PDF. In MS-QBI, the moment-like quantities are directly calculated from the signals on the multiple q-shells without calculating PDF. In our previous work we showed by simulations that the accuracy of the detected crossing angles in MS-QBI is higher than that in the conventional QBI for the same sampling number when the stabilities of the results are made to be approximately the same level. In this study we perform the fiber tracking of human brain based on MS-QBI and confirm the practicability of the method. We implement a simple procedure for streamline fiber trackings of pathways that encounter crossings.

Theory: We first consider the 1-dimensional case. The Fourier transform (FT) relationship between PDF and the signal intensity $S(q)$ is $S(q) = \int_{-\infty}^{\infty} P(R) e^{iqR} dR$, where R is the diffusion displacement and $P(R)$ is PDF. The n -th order moment of PDF is defined as $E(R^n) = \int_{-\infty}^{\infty} P(R) R^n dR$. Thus, we have $E(R^n) = \left(\frac{1}{i} \frac{d}{dq} \right)^n S(q) \Big|_{q=0}$, i.e., we can obtain the n -th order moment by knowing the n -th order differential coefficient of $S(q)$ at $q=0$, which can be known from the behavior of $S(q)$ when we change the q near zero (5). The 3-D FT relationship in the cylindrical coordinate is

$S(q_\rho, q_\theta, q_z) = \int_0^\infty dR_\rho \int_0^{2\pi} dR_\theta \int_{-\infty}^{\infty} dR_z R_\rho P(R_\rho, R_\theta, R_z) \exp[i\{q_\rho R_\rho \cos(R_\theta - q_\theta) + q_z R_z\}] \dots [1]$, where the subscripts ρ and θ denote the vector components of the radius and the azimuthal angle directions, respectively. By setting $q_z=0$ and $q_\rho=q$

(a radius of q-ball), and integrating out with respect to q_θ , we have $\int_0^{2\pi} S(q, q_\theta, 0) dq_\theta = \int_0^\infty dR_\rho \int_0^{2\pi} dR_\theta \int_{-\infty}^{\infty} dR_z R_\rho J_0(qR_\rho) P(R_\rho, R_\theta, R_z) \dots [2]$

where $J_0(\cdot)$ denotes the 0th order Bessel function. The quantity of the right-hand side of Eq. [2] is a value of the ODF for z -direction defined in the conventional QBI. The quantity is obtained as the left-hand side of the equation. This is the idea of the conventional QBI.

We consider the n -th derivative of Eq. [1] with respect to q_z , and then set q_z to zero and integrate out with respect to q_θ :

$$\left(\frac{1}{i} \frac{\partial}{\partial q_z} \right)^n \int_0^{2\pi} S(q, q_\theta, q_z) dq_\theta \Big|_{q_z=0} = \int_0^\infty dR_\rho \int_0^{2\pi} dR_\theta \int_{-\infty}^{\infty} dR_z R_\rho J_0(qR_\rho) P(R_\rho, R_\theta, R_z) R_z^n \dots [3].$$

The quantity of the right-hand side of Eq. [3] is a kind of n -th order moment of PDF with respect to R_z ; we define it as the value of ODF of our method. This quantity is obtained as the left-hand side of the equation, which can be known from the behavior of $\int_0^{2\pi} S(q, q_\theta, q_z) dq_\theta$, when we change the q_z near 0.

We use the second order moment ODF ($n=2$). The numerical implementation of the method is as follows. We assume that the diffusion have the inversion symmetry in any direction. Under the assumption, $\int_0^{2\pi} S(q, q_\theta, q_z) dq_\theta$ becomes an even function of q_z and a function of q_z^2 . In this case, we can reduce the left-hand side of Eq. [3] as $-2 \frac{\partial}{\partial q_z^2} \int_0^{2\pi} S(q, q_\theta, q_z^2) dq_\theta \Big|_{q_z=0}$,

which is approximated as $-\frac{2}{(\Delta q_z)^2} \int_0^{2\pi} \{S(q, q_\theta, \Delta q_z^2) - S(q, q_\theta, 0)\} dq_\theta$, where Δq_z is a new parameter. To calculate the ODF value in all orientations, signal samplings on two spherical shells are necessary. The radii of the shells are q and $\sqrt{q^2 + \Delta q_z^2}$ (Fig. 1).

Methods: A healthy adult male is scanned on a 1.5 T Philips Achieva MRI system using a multi-slice single-shot SE-EPI sequence. The matrix size is 128×128 . The FOV is $256 \text{ mm} \times 256 \text{ mm}$. The slice thickness is 2.0 mm. The number of the slice is 60 (gapless). The echo time is 88.4 ms. The number of signal averages is three. The radii of q-shells are, in terms of b value, 2200 and 3000 s/mm^2 . The duration and the separation of the diffusion gradient pulses are $\delta = 20 \text{ ms}$ and $\Delta = 43 \text{ ms}$, respectively (estimates based on measurements). The number of diffusion gradient directions is 32. The gradient direction table is obtained from Ref. (6). The tracking algorithm we use is a deterministic streamline one. We move a distance along a traveling direction from a starting point and repeat it. The traveling direction at a point is selected from the local maximum directions of an ODF averaged around the point. If multiple local maximum directions (i.e., fiber crossings) are found, we choose the direction nearest to the traveling direction at the previous point (**Step 1**). After a one line is traced, we then restart a tracking from a point at which the multiple local maxima have been detected, using another maximum direction (**Step 2**). For the **Step 2**, we select only the crossings that we are interested in from many crossings founded in the **Step 1**.

Results and Discussion: Figures 2-5 show the fiber tracking results of the pyramidal tract (PT). The trackings start from a starting region in the posterior limb of internal capsule. Figure 2 is the result of **Step 1**. Some traces are already described beyond the crossing with the superior longitudinal fasciculus (SLF) even in this step. All fiber crossings founded in the **Step 1** are drawn in Fig. 3 with the red lines. From the crossings we select the crossings that exist in the intersecting region with SLF, and then exclude the crossings whose directions are nearly perpendicular to the coronal section (Fig. 4). Figure 5 is the result of the **Step 2**. We can trace PT beyond the crossing with SLF. On the other hand, the distinction between PT and the corpus callosum in the corona radiata is still difficult.

References:

- Callaghan PT, MacGowan D, Packer KJ, Zelaya FO. J Magn Reson 1990; 90:177-182.
- Tuch DS. Magn Reson Med 2004;52:1358-1372.
- Zhan W, Yang Y. J Magn Reson 2006;183:193-202.
- Umezawa E, Yoshikawa M, Ohno K, Yoshikawa E, Yamaguchi K. Proc Intl Soc Mag Reson Med 16:1865, 2008.
- Umezawa E, Yoshikawa M, Yamaguchi K, Ueoku S, Tanaka E. Magn Reson Med Sci 2006;5:179-189.
- Farrell JA, http://godzilla.kennedykrieger.org/~jfarrell/software_web.htm

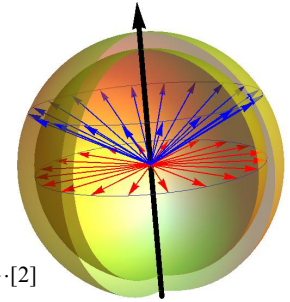


Fig. 1: Multi-shelled q-ball

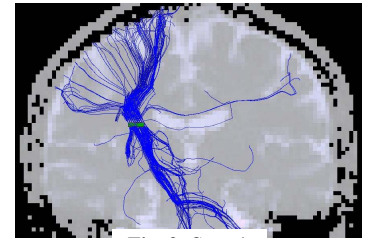


Fig. 2: Step 1

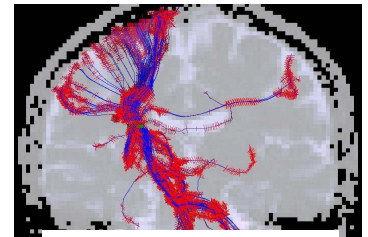


Fig. 3: All detected crossings

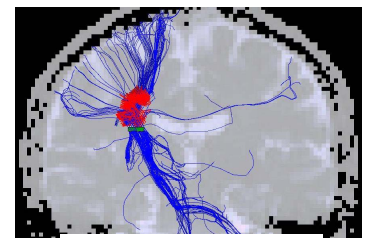


Fig. 4: Selected crossings

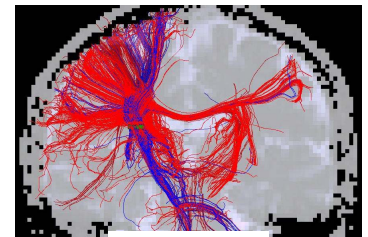


Fig. 5: Step 2